Journal of Structural Biology 163 (2008) 100–108

Contents lists available at ScienceDirect

Journal of Structural Biology

journal homepage: www.elsevier.com/locate/yjsbi

Spatial distribution of calcite and amorphous calcium carbonate in the cuticle of the terrestrial crustaceans *Porcellio scaber* and *Armadillidium vulgare*

Sabine Hild [a], Othmar Marti [b], Andreas Ziegler [a,*]

[a] Central Facility for Electron Microscopy, University of Ulm, Albert-Einstein-Allee 11, D89069 Ulm, Germany
[b] Department of Experimental Physics, University of Ulm, Albert-Einstein-Allee 11, D89069 Ulm, Germany

ARTICLE INFO

Article history:
Received 22 January 2008
Received in revised form 23 April 2008
Accepted 24 April 2008
Available online 3 May 2008

Keywords:
Amorphous calcium carbonate
Biomineralisation
Calcite
Confocal Raman microscopy
Crustacea
Cuticle
Isopoda

ABSTRACT

The crustacean cuticle is an interesting model to study the properties of mineralized bio-composites. The cuticle consists of an organic matrix composed of chitin–protein fibres associated with various amounts of crystalline and amorphous calcium carbonate. It is thought that in isopods the relative amounts of these mineral polymorphs depend on its function and the habitat of the animal. In addition to the composition, the distribution of the various components should affect the properties of the cuticle. However, the spatial distribution of calcium carbonate polymorphs within the crustacean cuticle is unknown. Therefore, we analyzed the mineralized cuticles of the terrestrial isopods *Armadillidium vulgare* and *Porcellio scaber* using scanning electron-microscopy, electron probe microanalysis and confocal μ-Raman spectroscopic imaging. We show for the first time that the mineral phases are arranged in distinct layers. Calcite is restricted to the outer layer of the cuticle that corresponds to the exocuticle. Amorphous calcium carbonate is located within the endocuticle that lies below the exocuticle. Within both layers mineral is arranged in rows of granules with diameters of about 20 nm. The results suggest functional implications of mineral distribution that accord to the moulting and escape behaviour of the animals.

1. Introduction

Mineralized biological composites have attracted increasing interest because of their outstanding mechanical properties that are well adapted to their biological function. Crustaceans are interesting models for the study of these materials. They have a protective exoskeleton, the cuticle, that also provides support to the muscles of the animals. The cuticle consists of an organic matrix containing chitin and sclerotised proteins, and a mineral phase with calcium carbonate as the main component. The organic matrix forms parallel chitin–protein fibres organised according to a twisted plywood model (Bouligand, 1972). In this model all fibres within a horizontal plane are parallel and continuously change their orientation from one plane to the next in a helicoidal manner. Recent studies have shown that, in the cuticle of some crustaceans considerable amounts of amorphous calcium carbonate (ACC) and, sometimes, of amorphous calcium phosphate (ACP) may be present in addition to calcite (Becker et al., 2005; Boßelmann et al., 2007; Levi-Kalisman et al., 2002; Neues et al., 2007; Wood and Russell, 1987). The occurrence of ACC within the cuticle is of particular interest. ACC is thought to play a role as a precursor of the crystalline calcium carbonate polymorphs (Aizenberg et al., 1996, 2002; Beniash et al., 1997; Hasse et al., 2000; Marxen et al., 2003; Raz et al., 2000; Weiss et al., 2002) and as transient reservoirs for calcium carbonate (Becker et al., 2003; Levi-Kalisman et al., 2002; Raz et al., 2002; Ziegler, 1994). The presence of ACC in conjunction with calcite within fully developed intermoult cuticles, however, suggests a specific function of ACC for the mechanical and chemical properties of the bio-composite.

A quantitative study on the mineral composition of dried tergite cuticles of *Porcellio scaber* and *Armadillidium vulgare* indicate 16%-wt and 12%-wt calcite and 38%-wt and 60%-wt ACC in addition to 27%-wt and 13%-wt organic material, respectively (Becker et al., 2005). Attempts were made to explain this difference by the diversity in the ecological strategies of these species. However, for a better understanding of the function of ACC and calcite within the cuticle, information of the spatial relation between these two mineral polymorphs would be essential. The current work on the micro-characterization of the material is limited to structural studies mostly of demineralised cuticle (Compère, 1991; Price and Holdich, 1980a; Strus and Blejec, 2001; Ziegler, 1997) or elemental analysis (Strus and Compere, 1996; Ziegler, 2002) that does not allow to distinguish between ACC and calcite. Recent studies have shown that Raman spectroscopy allows to differentiate between various calcium carbonate polymorphs including ACC (Weiner et al., 2003).

In an attempt to analyse the spatial distribution of calcite and ACC within the dorsal cuticle of *P. scaber* and *A. vulgare*, we employed field emission scanning electron-microscopy (FESEM), elec-

* Corresponding author. Fax: +49 (0) 731 502 3383.
E-mail address: andreas.ziegler@uni-ulm.de (A. Ziegler).

1047-8477/$ - see front matter © 2008 Elsevier Inc. All rights reserved.
doi:10.1016/j.jsb.2008.04.010

tron X-ray microprobe analysis (EPMA) and scanning confocal μ-Raman spectroscopic imaging (SCμ-RSI). Our results show for the first time that within the cuticle calcite and ACC are arranged in distinct layers with calcite located distally and ACC in the middle having only little overlap with the calcite layer. Such anisotropic distributions of mineral phases within bio-composites may have large effects on the mechanical properties of the cuticle as indicated by the differences between the species. These differences suggest that the mineral distribution evolved in accordance to eco-morphological defence strategies of terrestrial isopods.

2. Materials and methods

Porcellio scaber Latreille, 1804 and *Armadillidium vulgare* (Latreille, 1804) were collected from local biotopes, kept in plastic containers filled with soil and bark and fed with fresh potatoes, carrots and dry oak leaves. Animals in the intermoult stage were dissected in 100% methanol to obtain tergite samples. Previous studies have shown that ACC from sternal deposits of *P. scaber* is stable in methanol for at least 1 month (Becker et al., 2003). Soft tissue was carefully removed from the tergites and the sample washed first in bidistilled water for 2 s to remove salt residues and then in 100% methanol for at least 5 s to remove the water. Then the samples were air dried at room temperature and stored at −20 °C. Small pieces of the tergites were glued onto polymethylmetacrylate holders using superglue. Tergites were cut sagittally using a Reichert Ultracut ultramicrotome and glass knifes to obtain a plane surface. This surface was then polished with a diamond knife by successively advancing the specimen 15 times each by 70, 40 and 20 nm. Some samples were fractured in the sagittal plane to obtain cleaved instead of polished surfaces. For SEM analysis microtome polished and cleaved samples were rotary shadowed with 3 nm platinum (BAF 100, Balzers) at an angle of 45°. SEM micrographs were recorded with a field emission scanning electron-microscope (FESEM) (Hitachi S-5200) at an acceleration voltage of either 4 or 10 kV. For electron probe microanalysis (EPMA), the FESEM was equipped with an EDAX (Phönix) X-ray detector system with a 30 mm^2 SUTW window. Spectral maps were recorded at an acceleration voltage of 20 kV from microtome polished samples of high-pressure frozen (2.3×10^8 Pa; Compact 01, Wohlwend Engineering, Sennwald, CH) and freeze-dried tergites coated with a 10 nm-thick layer of carbon. Spectral maps (256×200 pixels) and lines scans (about 900 pixels) were recorded using a dwell time of 500 msec/pixel employing Genesis software (EDAX). Count rates were recorded between 1000–2000 s^{-1}. Besides high-pressure frozen and freeze-dried samples we also used samples dried and polished like those for the structural analysis (see above). No significant differences were detected in the elemental distribution between, on the one hand, the high-pressure frozen and freeze-dried cuticle samples and, on the other hand, the methanol-treated and air-dried ones.

A confocal Raman microscope (WITec, Ulm, Germany) equipped with a NdYag laser (wavelength of 532 nm) for excitation and a Nikon 100× (NA = 0.95) objective were used to locate calcite, ACC and organic matrix within the tergite cuticle by recording single Raman spectra and Raman spectral images. As reference material for the Raman measurements, calcite was precipitated from a solution containing 24 mmol L^{-1} Ca^{2+} and 24 mmol L^{-1} CO_3^{2-} at pH 8.6. Amorphous calcium carbonate without any organic additives was synthesized by a method described by Faatz et al. (2004) and biogenic ACC was obtained from the sternal ACC deposits of *P. scaber* (Becker et al., 2003; Ziegler, 1994). Purified chitin from crab-cuticle (Sigma–Aldrich) and bovine serum albumin (BSA) (VWR International) served as chitin and protein standards, respectively. The Raman spectra of the standards were recorded with integration times of 250 ms and 5 s. Sagittally cut and polished surfaces of the cuticles were prepared and analyzed in single imaging and in the Raman spectral imaging mode. To get high resolution Raman images, the samples were scanned point-by-point and line-by-line and Raman spectra between 0 and 3750 cm^{-1} were recorded with an integration time of 250 ms at every pixel (Pixel density: 10 spectra at 1 μm). Images were obtained analyzing the integral of specific bands above background employing the WITecProject_1_86 software (WITec, Ulm, Germany) (Schmidt et al., 2005). All images were colour-coded in a way that higher values of the integral sum, which correlate to a higher amount of a specific component, appear brighter.

3. Results

3.1. Structure of mineralized cuticle

The cuticle of isopods consists of four distinct layers described previously on the basis of TEM micrographs of demineralised cuticle samples: an outer epicuticle followed by an exocuticle, an endocuticle and an innermost membranous layer (Price and Holdich, 1980a; Strus and Blejec, 2001). In the mineralized cuticle of *P. scaber* several layers can be distinguished (Fig. 1A and B). The outermost layer is the about 200 nm-thick epicuticle (Fig. 1A) that also forms the plaques and tricorn sensilla of the cuticle (Price and Holdich, 1980b; Ziegler and Altner, 1995) and that is not mineralized. Just below the epicuticle lies a 1 μm-thick, outer mineralized layer of smooth appearance, which is part of the about 4 μm-thick exocuticle (Fig. 1A and B). Below the smooth layer the exocuticle appears rough and consists of a few poorly defined horizontal sublayers. These are a result of the helicoidal arrangement of stacked lamellae consisting of parallel chitin–protein fibrils (see Section 1). Proximally to the exocuticle lies the endocuticle that is about 15 μm-thick and contains many well-defined sublayers, each of about 1.5 μm-thick. The innermost membranous layer consists of about 0.35 μm-thick sublayers (Fig. 1A). Here, the number of sublayers varies considerably among samples. This is probably due to incomplete synthesis of the membranous layer in some of the samples. High resolution micrographs indicate that the outer smooth layer consists of densely fused granules of about 20-nm diameter that form oblique sheets (Fig. 1C). Cleaved surfaces of the endocuticle appear rough and mineralized bundles of various orientations are visible (Fig. 1D). Ultra-microtome polished surfaces reveal that the endocuticle comprise long rows of 10–15 nm-thick mineral granules. (Fig. 1E and F). Parabolic patterns due to the helicoidal arrangement of stacked layers that are known from TEM studies of arthropod cuticles are also visible (Fig. 1E) and indicate that the granules are aligned along parallel chitin–protein fibres.

The cuticle of *A. vulgare* is more than 40 μm-thick (Fig. 2A). It consists of a thin distal epicuticle, an exocuticle, an endocuticle and a membranous layer that are about 10, 30 and 5 μm-thick, respectively. The distal 0.6 μm-thick region of the exocuticle consists of oblique sheets composed of rows of 20 nm-thick granules (Fig. 2C) forming a smooth layer similar to that of *P. scaber* (Fig. 2B and C). About 2–3 μm below this layer, the cuticle appears rough and very dense, and sublayers are not well defined (Fig. 2B). Proximally to this transition zone, sublayers of the exocuticle are visible (Fig. 2A and B) and the cleaved surfaces have a blocky appearance with bundles of fibres composed of 20 nm granules (Fig. 2D and E) and probably chitino-protein fibres (Romano et al., 2007). Within the endocuticle sublayers of helicoidally arranged stacks of parallel fibres are visible (Fig. 2F). From the distal side of the endocuticle to the proximal side of the membranous layer the thickness of the sublayers continuously decreases from 3 to about 0.3 μm (Fig. 2A).

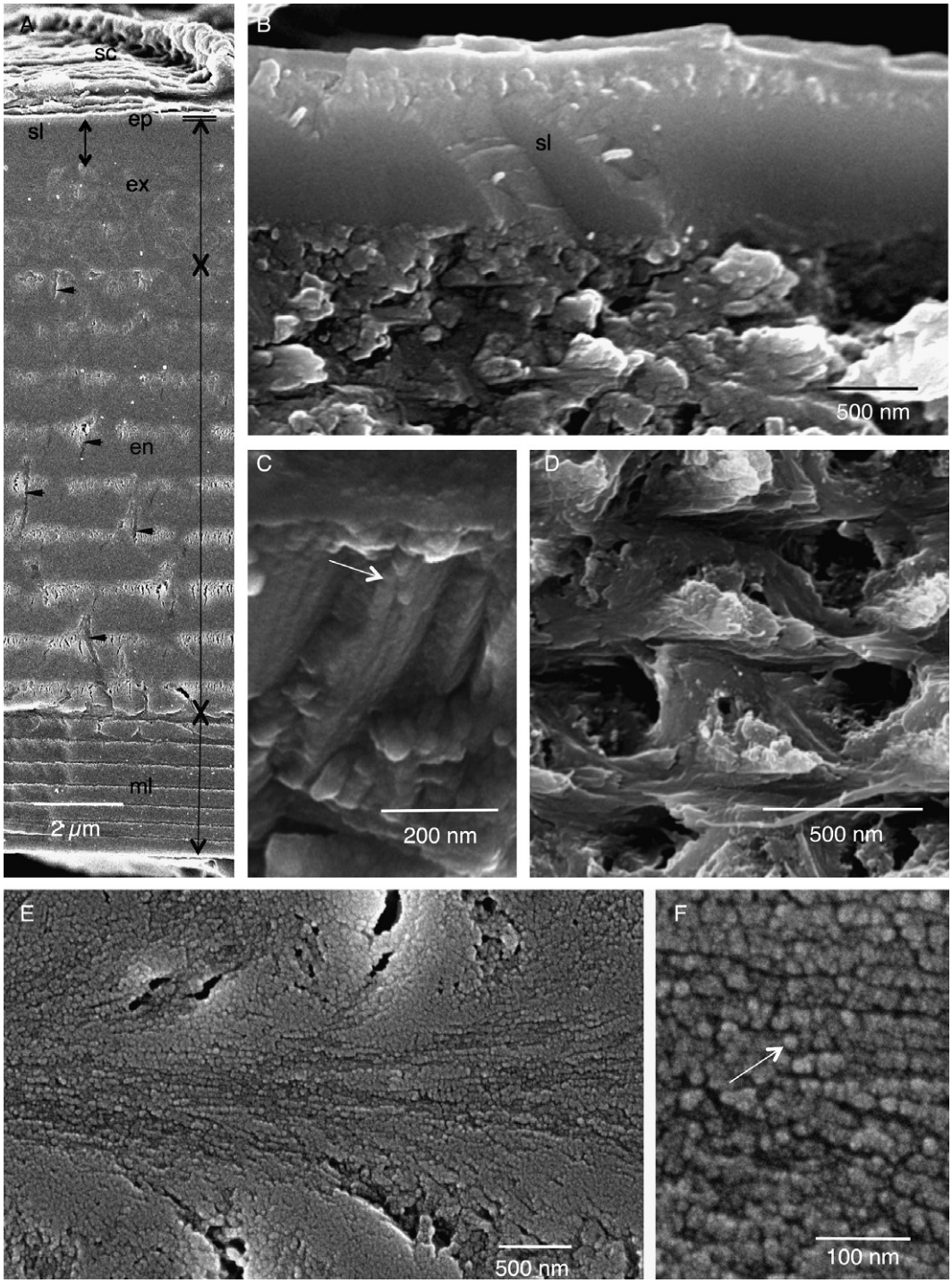

Fig. 1. Field-emission scanning electron-microscopy of sagittally cleaved mineralized tergite cuticle of *Porcellio scaber*. (A) Overview of a microtome polished surface. The cuticle consists of a thin distal epicuticle (ep) that forms the scales (sc), a mineralized exocuticle (ex) that comprises a distal smooth layer (sl), a mineralized endocuticle (en) and a membranous layer (ml). Pore channels (arrowheads) are in particular visible within the endocuticle (en). (B) Structure of distal region of the exocuticle showing smooth fracture surfaces. (C) High resolution image of the smooth layer showing oblique layers composed of fused 20 nm thick granules. (D) Structure of the endocuticle. (E and F) High resolution images of microtome polished surface of the endocuticle showing 20-nm diameter granules aligned along chitin–protein fibrils of the cuticle.

3.2. Mineral distribution within the cuticle

Electron X-ray microprobe analysis (EPMA) and scanning confocal μ-Raman spectroscopic imaging (SCμ-RSI) requires that the surface of the specimen have a smooth and planar surface. Field emission scanning electron-microscopy (FESEM) shows that these conditions are well met by the microtome polished cuticle surfaces (Fig. 1A). After washing the microtome polished specimen for 15 min in methanol, the surfaces are clean and no wear debris are to be found on the surfaces (Fig. 1E and F).

Elemental maps of sagittal surfaces of the mineralized cuticle of *P. scaber* and *A. vulgare* are shown in Fig. 3. X-ray spectra of the cuticles reveal the presence of magnesium and phosphorus in addition to the expected carbon, oxygen and calcium peaks (Fig. 3A and E). Elemental maps and line scans show that the calcium content within the cuticle of both *P. scaber* and *A. vulgare* is highest at

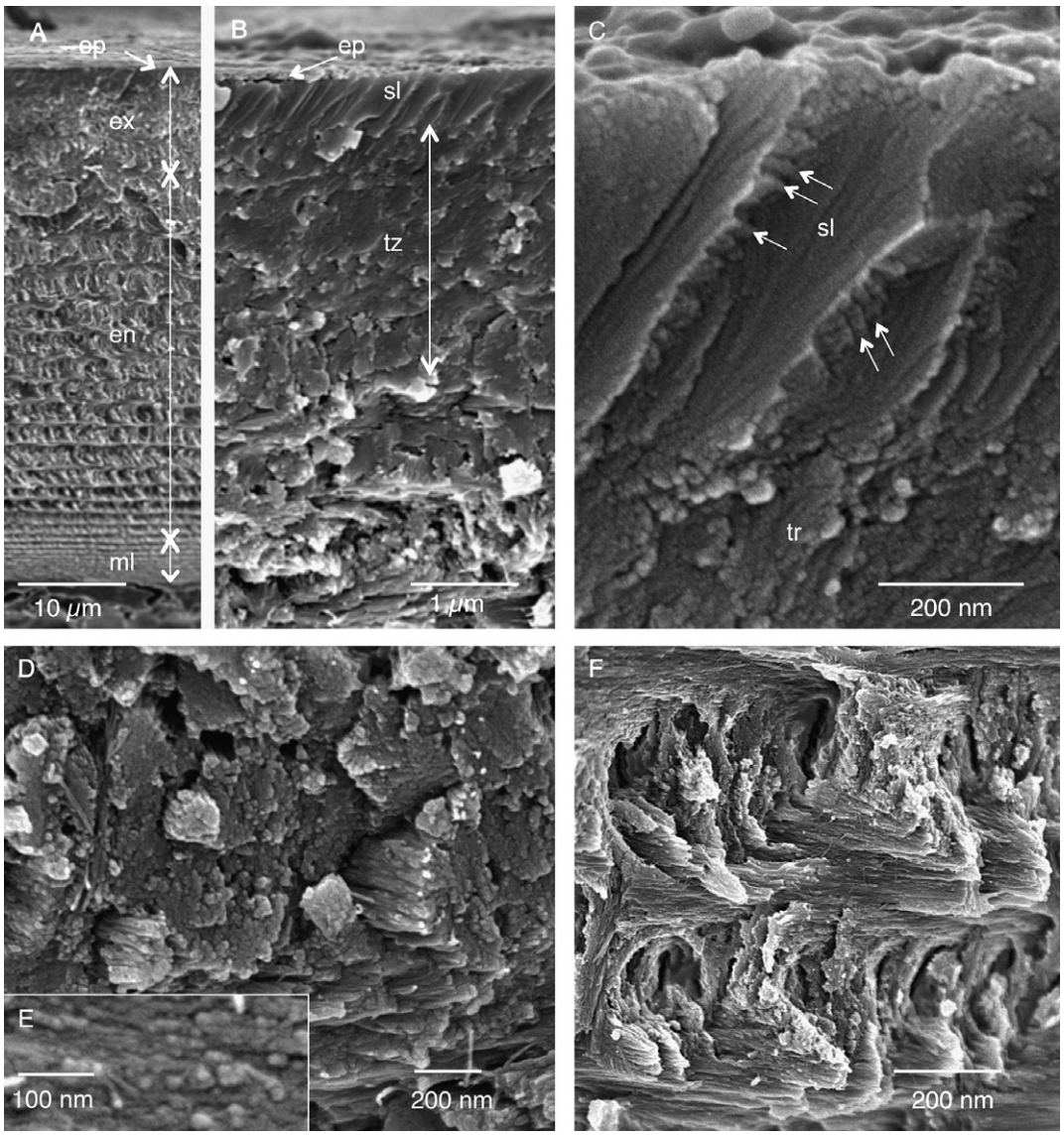

Fig. 2. Field-emission scanning electron-microscopy of sagittally cleaved mineralized tergite cuticle of *Armadillidium vulgare*. (A) Overview showing a thin distal epicuticle (ep), a mineralized exocuticle (ex), a mineralized endocuticle (en) and a membranous layer (ml). (B) Structure of distal region of the exocuticle showing a distal smooth layer (sl) and a transition zone that appears rough and dense (tz). (C) High resolution micrograph of the smooth layer showing oblique sheets composed of rows of 20 nm-thick granules (arrows). (D and E) Surfaces of the exocuticle have a blocky appearance with bundles of fibres composed of 20-nm granules. (F) Helicoidally arranged stacks of parallel fibres within the endocuticle.

the distal side of the cuticle and declines moderately towards the middle part of the cuticle. At the proximal side the calcium content decreases towards the unmineralized membranous layer (Fig. 3B and F). The magnesium content in the cuticle of *P. scaber* and *A. vulgare* is almost homogeneous with the exception of an area within the proximal part of the mineralized cuticle in which the magnesium is higher (Fig. 3C and G). The phosphorus content in the cuticle of both species is low in the distal region and gradually increases towards a plateau in the middle of the cuticle (Fig. 3D and H). A layer with high phosphorus content is present within the proximal region of the mineralized part of the cuticle. The membranous layer contains only a small amount of phosphorus.

Raman spectra of both calcite and ACC standards (Fig. 4A–C) show bands assigned to carbonate stretching vibrations having their maxima at 1086 and 1080 cm^{-1}, respectively. Distinct lattice vibrations at 158 and 280 cm^{-1} occur for calcite only (Fig. 4A), whereas, for ACC the two peaks are replaced by a single broad band ranging from 100 to 300 cm^{-1} (Fig. 4B and C). These differences in the spectra allow the discrimination between the different calcium carbonate polymorphs. To obtain Raman spectral images of the distribution of total calcium carbonate, the integral values of the spectral area ranging from 1070 to 1100 cm^{-1} (Fig. 4), that includes the carbonate band, are recorded and plotted in *x-y* coordinates. Resulting Raman spectroscopic images indicate that in both species calcium carbonate occurs within the whole exo- and endocuticle (Fig. 5A and F). The inner membranous layer appears to be virtually devoid of calcium carbonate. Plotting the integral values of the spectral area ranging from 200 to 300 cm^{-1} corresponding to the calcite lattice vibration at 280 cm^{-1} reveals the local distribution of calcite only (Fig. 5B and G). Virtually, calcite is restricted to the distal fifth of the cuticle.

Performing Raman spectral line scans (Fig. 5D and I) allows a more detailed analysis. The carbonate signal is in particular strong within the distal fifth of the cuticle, about 4 μm thick in *P. scaber* and about 8 μm thick in *A. vulgare*. This area also corresponds to the distribution of calcite. Proximally the signal decreases to intermediate intensities and no significant change can be found within the next 12 and 30 μm in *P. scaber* and *A. vulgare*, respectively. To-

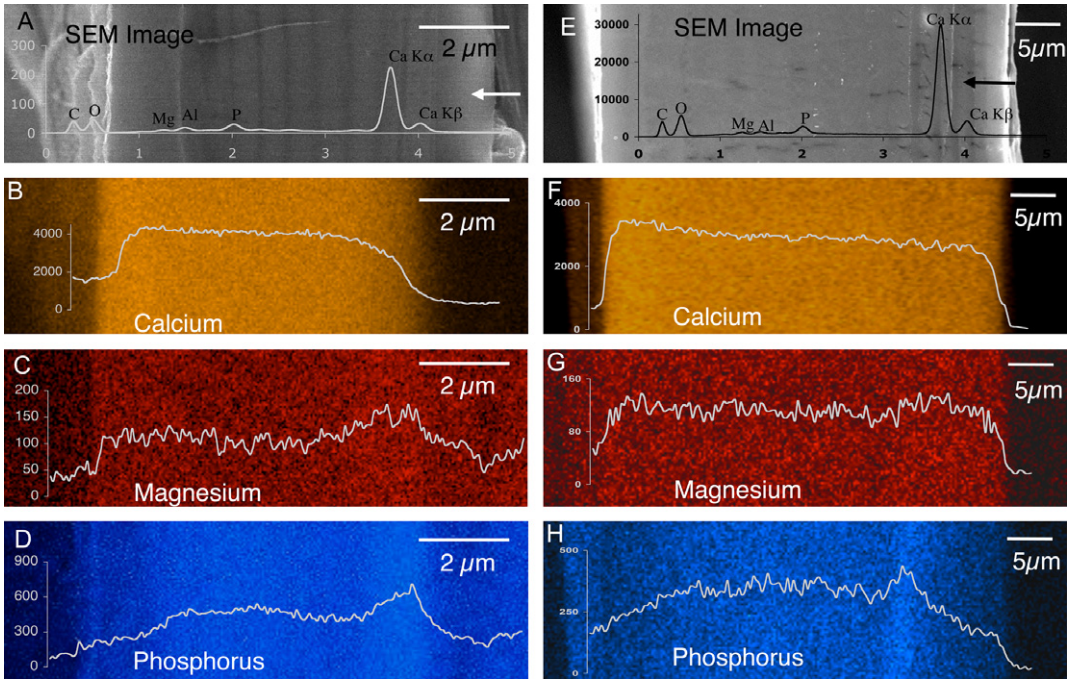

Fig. 3. Electron probe microanalysis (EPMA) of sagittally cleaved and microtome polished surfaces of the mineralized high-pressure frozen and freeze-dried tergite cuticles of *Porcellio scaber* (A–D) and *Armadillidium vulgare* (E–H). (A and E) SEM image and elemental X-ray spectrum indicate the presence of C, O, Mg, P and Ca. The aluminium peak is due to the use of the conductive glue at the sides of the specimen. Spectral maps and line scans are shown for calcium (B and F), magnesium (C and G) and phosphorus (D and H). The arrows in (A) and (B) indicate the position from which line scans were recorded.

wards the membranous layer the signal declines to background levels. From single Raman spectra recorded within the region of the highest carbonate signal (Fig. 5E and J) it can be concluded that here both calcite and ACC is present. Thus, the exocuticle contains both ACC and calcite, whereas only ACC is present within the endocuticle (Fig. 5E and J). Besides the calcium carbonate bands, all of the spectra (Fig. 5E and J) taken in the mineralized area show additional bands in the range between 2800 and 3100 cm^{-1} that can be assigned to CH-stretching vibrations (Fig. 4D and E). Thus, imaging the integral of this spectral area (Fig. 4) results in maps of the distribution of the organic matrix (Fig. 5C and H). A thin layer of organic material can be seen at the distal side of the cuticle corresponding to the epicuticle. Due to limits in spatial resolution the epicuticle appears broadened with some overlap of the carbonate and calcite signal (Fig. 5C–I). However, distinct calcite crystals are virtually lacking within the epicuticle. In the single spectra (Fig. 5E and J) taken within this area only a small amide peak at 3275 cm^{-1} is visible, whereas the peak at 3450 cm^{-1} that characteristic of hydrogen bonds in chitin is missing. This suggests the presence of proteins and possibly long functionalised alkanes (waxes) within the epicuticle, in accordance with earlier studies on isopod epicuticle (Compère, 1991). In both species the signal for the organic component in the exo- and endocuticle increases (Fig. 5D and I) from the distal to the proximal side with a particularly strong intensity within the unmineralized, membranous layer. Single spectra recorded within these areas (Fig. 5E and J) show a double band with maxima at 3275 and 3450 cm^{-1}, respectively, that is characteristic for chitin (Table 1) (Galat and Popowicz, 1978). Sinusoidal variations in the intensity of the organic signal (Fig. 5D and I) correspond to helicoidally arrangement of stacked lamellas of protein–chitin fibrils.

4. Discussion

For the first time the present paper reports the spatial distribution of ACC and calcite within the cuticle of crustaceans. The study furthers previous work on quantitative aspects of tergite mineral composition in *A. vulgare* and *P. scaber* (Becker et al., 2005). By using scanning confocal µ-Raman spectroscopy our results indicate that the tergal cuticle of terrestrial isopods contain a thin distal layer of calcite and a proximal layer of amorphous calcium carbonate (ACC). The distribution of different calcium carbonate polymorphs corresponds well to features of the mineralized cuticle. It suggests facilitation of ACC resorption in premoult and early stabilisation of the external part of the new cuticle by calcite after ecdysis.

The epicuticle of Crustacea contains no helicoidally arranged chitin–protein fibres. It contains proteins (Skinner et al., 1992) and waxy layers that, in terrestrial isopods, are thought to act as surface waterproofing barriers reducing the tegumental water loss (Compère, 1991; Hadley and Warburg, 1986). Our Raman spectroscopic results are in accordance with the presence of proteins and waxes. In the inner epicuticle of the decapod species *Cancer pagurus* and *Carcinus maenas,* calcite crystals have been found within cuticular pores that end just underneath the outer epicuticle (Hegdahl et al., 1977; Roer and Dillaman, 1984). Raman spectroscopic imaging of the cuticle of *P. scaber* and *A. vulgare* show no indications of epicuticular calcite crystals. Although the epicuticle appears broadened in the Raman images due to limits in spatial resolution, calcite containing pore channels should be visible since empty pore channels are well resolved in mineralized layers of the cuticle. Although we have no clear indication of the presence of proteins within the unmineralized membranous layer, small amounts of protein cannot be excluded. The high amount of chitin within this layer is in agreement with studies on the organic material in the membranous layer of *C. pagurus* that contains proteins and 74% chitin (Welinder, 1975).

In *P. scaber* and *A. vulgare* the distribution of calcite within the cuticle corresponds well with the dimensions of the exocuticle, whereas the calcite free regions that contain ACC only correspond well with that of the endocuticle. The mineralized exocuticle of both species contains a peculiar distal structure of smooth appear-

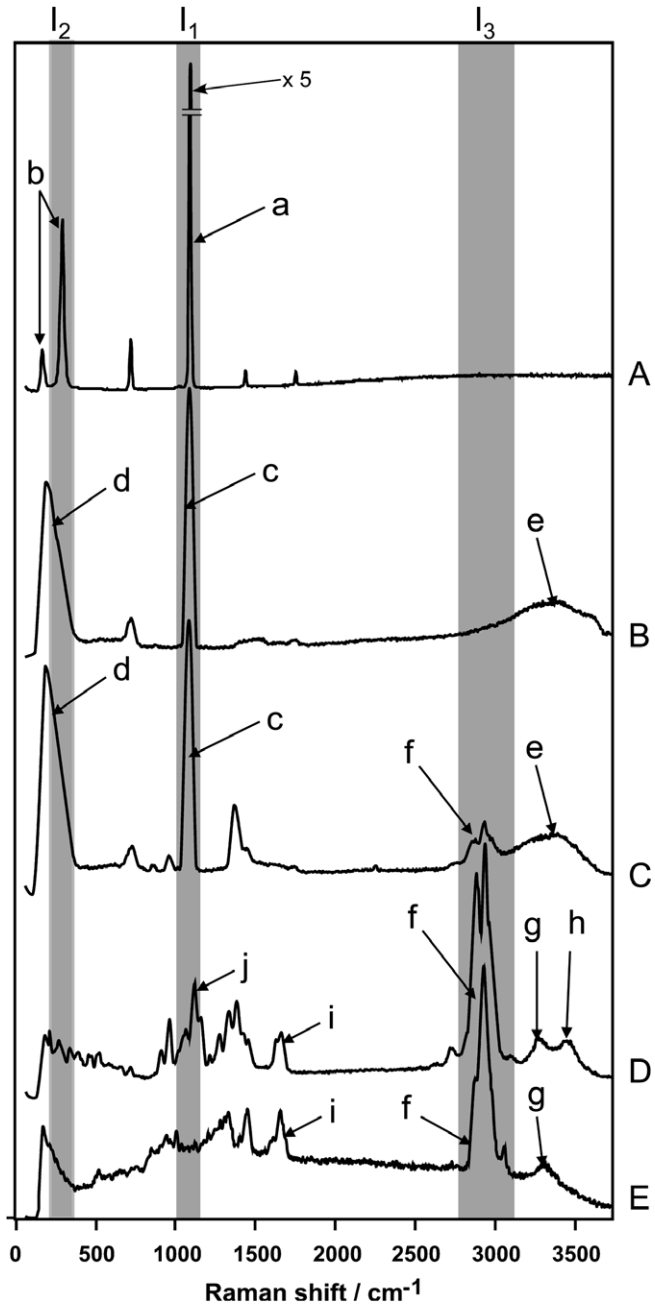

Fig. 4. Raman spectra for calcite (A), synthetic ACC (B), ACC from the sternal deposits of *P. scaber* (C), crab chitin (D) and bovine serum albumin (BSA) (E). Characteristic bands indicated by a–j are explained in Table 1. Integral areas used for recording the Raman images are indicated in grey (I_1 = total carbonate; I_2 = calcite,; I_3 = organic material).

ance that contains calcite, a low amount of phosphorus and organic material (see below). The dense structure of this smooth layer suggests that it may be harder and less ductile than the more proximal layers that appear less dense. It also seems possible that the dense structure of the smooth layer provides a way to reduce water loss contributing to the water proofing function of the epicuticle (see above). It is of interest that the mineral within the endo- and exocuticle is composed of granular structures probably lined along the chitin–protein fibrils. Within the distal smooth region of the exocuticle of *P. scaber* and *A. vulgare* the calcite granules are similar in appearance to calcite granules observed in sodium hypochlorite treated endocuticles of the decapod crustaceans *C. maenas* and *Menippe mercenaria* (Roer and Dillaman, 1984) appearing aligned to cuticular filaments and densely packed forming rod-like superstructures. However, the granules differ in their diameters that are at least three times larger in the decapod endocuticles as compared to those in isopods. Furthermore, within the endocuticle of isopods, the connections between adjacent ACC granules appear rather loose. As already mentioned in the Section 1, an important function of ACC in invertebrate bio-composites is its role as a precursor of crystalline calcium carbonate. The similarities of the calcite granules within the exocuticle and ACC granules within the endocuticle of the isopods raise the possibility that during mineralization of the most distal layers, calcite granules are first precipitated as amorphous precursors that form later mesocrystalline aggregates. Such a transition from 10–15 nm-thick ACC granules into calcite mesocrystals has been demonstrated in vitro during formation of nacre-type calcite layers (Volkmer et al., 2005). In addition, such a transition was also proposed recently for the cuticle of the dorsal carapace of *Callinectus sapidus,* based on observation on the solubility of cuticular calcium carbonate just after its deposition (Dillaman et al., 2005).

The present study confirms directly previous studies in which a high abundance of ACC within the cuticle was predicted on the base of indirect measurements (Becker et al., 2005; Neues et al., 2007). A comparative study on the composition of the cuticles of four marine and six terrestrial isopods has shown that the composition of the tergite cuticle varies between species and depends on habitat and escape behaviour of the animal (Neues et al., 2007). For the terrestrial species the reason for the difference in cuticle composition may be due to their mineral storage strategy that was probably evolved during the transition from marine to terrestrial habitats to compensate for the slow uptake of calcium ions in a terrestrial environment. During moulting, terrestrial isopods are subject to a cycle of resorption and recycling of cuticular calcium that is stored in peculiar sternal ACC deposits (Becker et al., 2003; Steel, 1993; Ziegler, 1994; Ziegler et al., 2007). Since ACC is about 10 times more soluble than crystalline calcium carbonate polymorphs (Brecevic and Nielson, 1989), the presence of high amounts of ACC facilitates resorption of calcium carbonate from the premoult cuticle, and thus storage and recycling of the mineral. Within this context the distribution of ACC within the proximal layers of the

Table 1
Characteristic Raman shifts of the main cuticle components

	Group	Characteristic wavenumber/cm^{-1}	Reference
a	Calcite CO_3 stretching	1086	Rutt and Nicola (1974)
b	Calcite lattice vibration	186 and 280	Rutt and Nicola (1974)
c	ACC CO_3 stretching	1077	Tlili et al. (2001)
d	ACC lattice vibrations	100–300	Tlili et al. (2001)
e	H_2O stretching	3000–3500	Tlili et al. (2001)
f	CH stretching	2800–3020	Tlili et al. (2001)
g	Amide	3275	Galat and Popowicz (1978)
h	Hydrogen bonds (O–H, N–H)	3450	Galat and Popowicz (1978)
i	Amide I; Amide II	1550, 1625	Galat and Popowicz (1978)
j	ν(C–O), ν(C–C), ν(C–N)	1045, 1090, 1105, 1125	Galat and Popowicz (1978)

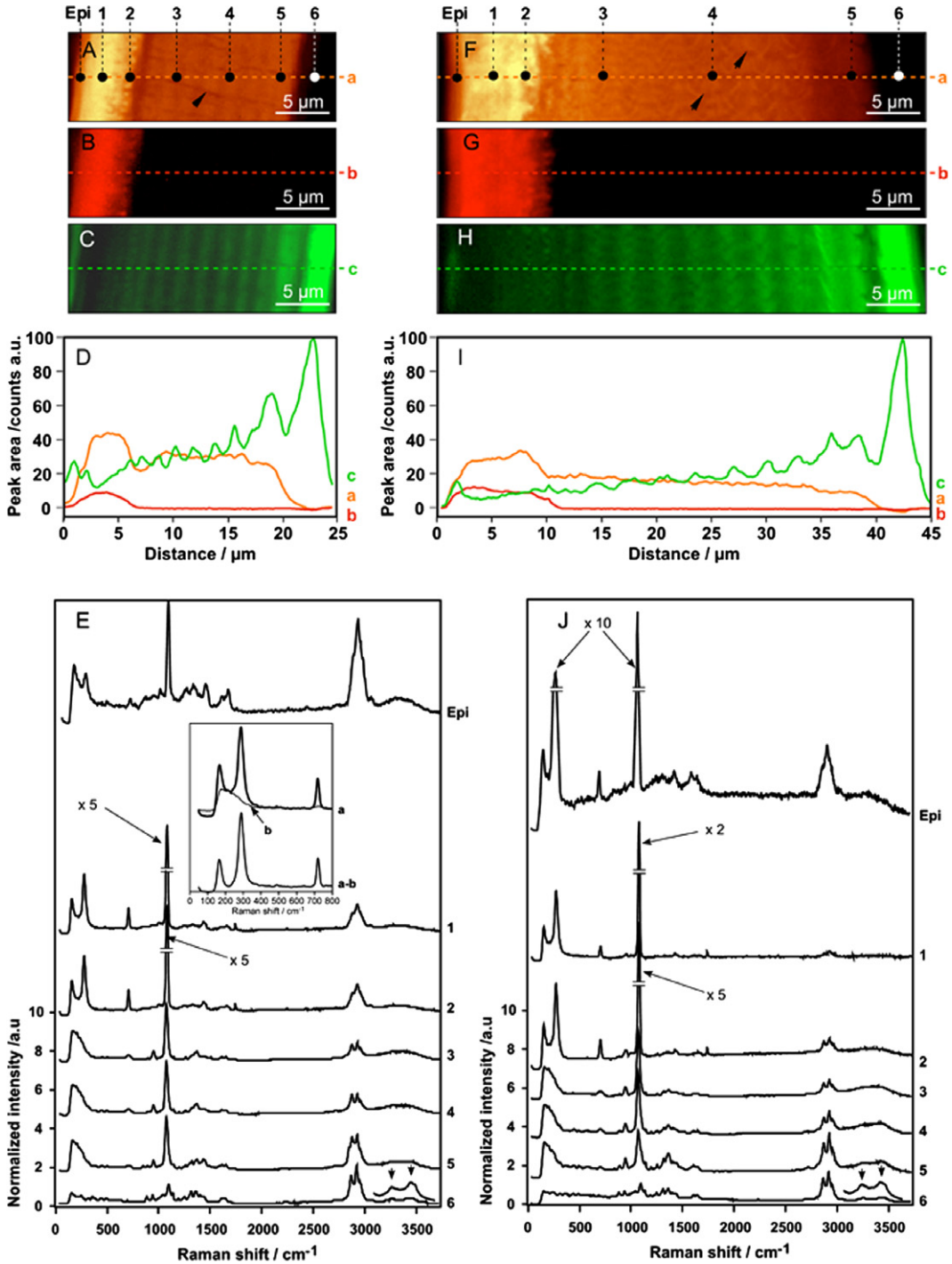

Fig. 5. Raman spectroscopic images (A–C and F–H), line scans (D and I) and single spectra (E and J), recorded from a sagittally cleaved and microtome polished surface of the mineralized tergite cuticles of *Porcellio scaber* (A–E) and *Armadillidium vulgare* (F–J), show the local distribution of the various components. Calcium carbonate (A and F) occurs within the whole exo- and endocuticle, whereas calcite (B and G) is located within the exocuticle only. Pore channels (arrowheads) appear devoid of mineral. The amount of organic material (C and H) increases from the distal to the proximal region of the cuticle. The membranous layer is devoid of calcium carbonate. Dotted lines in the Raman images (A and F) indicate the position where the line scans are recorded for a: carbonate, b: calcite and c: organic material to determine material distribution. Points Epi and 1–6 correspond to the positions where the single spectra (E and J) were recorded. The inset in E shows recording 1, the normalized control spectrum of ACC and the difference between these spectra, between 0 and 800-cm^{-1}, indicating the presence of both calcite and ACC within the exocuticle. Small arrowheads in (E and J) point to bands at 3275-cm^{-1} and 3450-cm^{-1}.

cuticle makes perfect sense. The proximal layers are demineralised before moulting to allow for calcium ions storage, while distal layers should remain calcified within the cuticle to provide some protection until shedding of the cuticle. Furthermore, the distal calcite layer supplies some stability to the exuviae from which the animal has to come out of. This may allow firm separation of the old from soft new cuticle facilitating shedding of the exuviae. Furthermore, larger amounts of mineral within the cuticle probably require larger reservoirs allowing storage of larger fractions of the cuticular mineral during moulting. Thus the thicker layer of ACC within the cuticle of *A. vulgare* as compared to that of *P. scaber* suggests that ACC rather than calcite is resorbed from the cuticle. This is

confirmed by a current study on mineral composition within tergites of *P. scaber* during various moulting stages that also suggest resorption of ACC but not calcite from the cuticle (Neues et al. 2008, manuscript in preparation).

Terrestrial isopods can be grouped by their skeletal construction into categories that are correlated to ecological strategies and behavioural patterns (Schmalfuss, 1984). Species like *P. scaber,* which avoid predation by running away or clinging to a substrate protecting the soft ventral surface of the body, require a more or less thin and somewhat flexible cuticle that contains moderate amounts of mineral. On the contrary, species like *A. vulgare* that avoid predation by rolling into a perfect sphere require a thick and inflexible cuticle that is strongly mineralised. This difference in behaviour may explain the higher relative amount of ACC within the cuticle of *A. vulgare* versus that of *P. scaber*.

Considerable amounts of phosphorus and magnesium are found in the cuticle of virtually all crustaceans (Compère and Goffinet, 1987; Fieber and Lutz, 1985; Greenaway, 1985; Vijayan and Diwan, 1996; Ziegler, 2002). An indirect approach for the quantification of amorphous calcium phosphate (ACP) within the cuticle of *P. scaber* and *A. vulgare* yielded 12%-wt and 11%-wt ACP, respectively (Becker et al., 2005). Within biological tissues, phosphorus occurs as phosphate either in an organic form like phospholipids and phosphorylated proteins, or in the form of calcium phosphate. In vitro experiments have shown that, under physiological conditions, low concentrations of phosphate prevent calcite crystal nucleation and formation (Bachra et al., 1963; Reddy, 1977). Thus, the correlation between phosphorus and ACC within the present study raises the possibility that phosphate supports ACC formation during mineral precipitation.

It seems that in the tergite cuticles of the two species no large difference in the magnesium content occurs between regions containing calcite and those that contain ACC. In a previous study it was shown that within the tergite cuticle of *P. scaber* and *A. vulgare,* about 18% and 12% of the magnesium is located within the calcite crystal lattice, respectively (Becker et al., 2005), in good agreement with our finding of magnesium within the distal part of cuticle. Magnesium within the calcite crystal lattice may have an effect on the mechanical properties of the cuticle since magnesium calcite is harder than calcite without magnesium (Becker et al., 2005). Magnesium ions are also known to stabilize ACC (Aizenberg et al., 2002; Loste et al., 2003) supporting our assumption that the calcite layer within the tergite cuticle has formed from amorphous precursor phases (see above). Clearly, the issue of ACC as a precursor phase within crustacean cuticles requires further exploration.

The most fascinating question raising from this study is, how isopods control the local precipitation of calcite and ACC, and how the amorphous state of calcium carbonate is stabilized. It appears likely that precipitation and crystallisation of calcium carbonate is under the control of cuticular proteins. Recent studies suggest that specific proteins from the exoskeleton (Endo et al., 2004; Inoue et al., 2001; Sugawara et al., 2006) and from calcium carbonate storages sites (Takagi et al., 2000; Testenière et al., 2002) provide nucleation sites for ACC or calcite, prevent mineral precipitation, or stabilize amorphous calcite precursors. Furthermore, protein extracts from the cuticle of the decapod crustacean *C. sapidus,* that have large effects on in vitro mineral precipitation, change its protein composition from pre to post ecdysis (Coblentz et al., 1998; Shafer et al., 1995). This has lead to a model in which some proteins provide calcite nucleation sites while others can mask these sites until deactivation. Deactivation of these nucleation inhibitory proteins would then expose the nucleation sites leading to mineral precipitation (Coblentz et al., 1998). The situation in terrestrial isopods, with two distinct mineral phases within their cuticle, makes regulation of mineral precipitation even more complex. Apparently, isopods are able to regulate not just mineral precipitation, possibly by a similar mechanism as described for the decapods model (Coblentz et al., 1998), but are also able to regulate formation of calcite and ACC within distal and proximal regions of the cuticle, respectively. This is probably brought about by crystallization of ACC precursors within the distal region and prevention of crystallisation in the proximal region of the cuticle. The amorphous state of calcium carbonate granules is probably stabilized by ions and/or one or several components of the organic matrix. For isopods, evidence for ACC stabilisation by organic components was provided by an ultrastructural investigation of the sternal ACC deposits of *P. scaber* during natural degradation (Fabritius and Ziegler, 2003). Further investigations on the matrix proteins of the cuticle are required to understand the mechanisms for ACC stabilisation and crystallisation within the isopod cuticle.

Acknowledgement

This work was supported by the Deutsche Forschungsgemeinschaft within the research program "Principles of Biomineralisation" SPP 1117 (Zi 368/4-3).

References

Aizenberg, J., Lambert, G., Addadi, L., Weiner, S., 1996. Stabilization of amorphous calcium carbonate by specialized macromolecules in biological and synthetic precipitates. Adv. Mater. 8, 222–226.

Aizenberg, J., Lambert, G., Weiner, S., Addadi, L., 2002. Factors involved in the formation of amorphous and crystalline calcium carbonate: a study of an ascidian skeleton. Am. Chem. Soc. 124, 32–39.

Bachra, B.N., Trautz, O.R., Simon, S.L., 1963. Precipitation of calcium carbonates and phosphates. I. Spontaneous precipitation of calcium carbonates and phosphates under physiological conditions. Arch. Biochem. Biophys. 103, 124–138.

Becker, A., Ziegler, A., Epple, M., 2005. The mineral phase in the cuticles of two species of Crustacea consists of magnesium calcite, amorphous calcium carbonate, and amorphous calcium phosphate. Dalton Trans. 2005, 1814–1820.

Becker, A., Bismayer, U., Epple, M., Fabritius, H., Hasse, B., Shi, J., Ziegler, A., 2003. Structural characterisation of X-ray amorphous calcium carbonate (ACC) in sternal deposits of the Crustacea *Porcellio scaber*. Dalton Trans. 2003, 551–555.

Beniash, E., Aizenberg, J., Addadi, L., Weiner, S., 1997. Amorphous calcium carbonate transforms into calcite during sea urchin larval spicule growth. Proc. R. Soc. London. B 264, 461–465.

Boßelmann, F., Romano, P., Fabritius, H., Raabe, D., Epple, M., 2007. The composition of the exoskeleton of two crustacea: the american lobster *Homarus americanus* and the edible crab *Cancer pagurus*. Thermochim. Acta 463, 65–68.

Brecevic, L., Nielson, A.E., 1989. Solubility of amorphous calcium carbonate. J. Cryst. Growth 98, 504–510.

Bouligand, Y., 1972. Twisted fibrous arrangement in biological materials and cholesteric mesophases. Tissue Cell 4, 189–217.

Coblentz, F.E., Shafer, T.H., Roer, R.D., 1998. Cuticular proteins from the blue crab alter in vitro calcium carbonate mineralization. Comp. Biochem. Physiol. Part B 121, 349–360.

Compère, P., 1991. Fine structure and elaboration of the epicuticle and the pore canal system in tergite cuticle of the land isopod *Oniscus asellus* during a moulting cycle. In: Juchault, P., Mocquard, J.P. (Eds.), The Biology of Terrestrial Isopods III. Université de Portiers, pp. 169–175.

Compère, P., Goffinet, G., 1987. Elaboration and ultrastructural changes in the pore canal system of the mineralized cuticle of Carcinus maenas during the moulting cycle. Tissue Cell 19, 859–875.

Dillaman, R., Hequembourg, S., Gay, M., 2005. Early pattern of calcification in the dorsal carapace of the blue crab, *Callinectes sapidus*. J. Morphol. 263, 356–374.

Endo, H., Takagi, Y., Ozaki, N., Kogure, T., Watanabe, T., 2004. A crustacean Ca^{2+}-binding protein with a glutamate-rich sequence promotes $CaCO_3$ crystallization. Biochem. J. 384, 159–167.

Faatz, M., Gröhn, F., Wegner, G., 2004. Amorphous calcium carbonate: synthesis and potential intermediate in biomineralization. Adv. Mater. 16, 996–1000.

Fabritius, H., Ziegler, A., 2003. Analysis of $CaCO_3$ deposit formation and degradation during the molt cycle of the terrestrial isopod *Porcellio scaber* (Crustacea, Isopoda). J. Struct. Biol. 142, 281–291.

Fieber, L.A., Lutz, P.L., 1985. Magnesium and calcium metabolism during molting in the freshwater prawn *Macrobrachium rosenbergii*. Can. J. Zool. 63, 1120–1124.

Galat, A., Popowicz, J., 1978. Study of the Raman scattering spectra of chitins. Biochemistry 26, 519–524.

Greenaway, P., 1985. Calcium balance and moulting in the Crustacea. Biol. Rev. 60, 425–454.

Hadley, N.F., Warburg, M.R., 1986. Water loss in three species of xeric-adapted isopods: correlations with cuticular lipids. Comp. Biochem. Physiol. 85A, 669–672.

Hasse, B., Ehrenberg, H., Marxen, J.C., Becker, W., Epple, M., 2000. Calcium carbonate modifications in the mineralized shell of the freshwater snail *Biomphalaria glabrata*. Chem. Eur. J. 6, 3679–3684.

Hegdahl, T., Gustavsen, F., Silness, J., 1977. The structure and mineralization of the carapace of the crab (*Cancer pagurus* L.). Zool. Scripta 6, 215–220.

Inoue, H., Ozaki, N., Nagasawa, H., 2001. Purification and structural determination of a phosphorylated peptide with anti-calcification and chitin-binding activities in the exoskeleton of the crayfish *Procambarus clarkii*. Biosci. Biotechnol. Biochem. 65, 1840–1848.

Levi-Kalisman, Y., Raz, S., Weiner, S., Addadi, L., Sagi, I., 2002. Structural differences between biogenic amorphous calcium carbonate phases using X-ray absorption spectroscopy. Adv. Funct. Mater. 12, 43–48.

Loste, E., Wilson, M., Seshadri, R., Meldrum, F.C., 2003. The role of magnesium in stabilising amorphous calcium carbonate and controlling calcite morphologies. J. Cryst. Growth 254, 206–218.

Marxen, J.C., Becker, W., Finke, D., Hasse, B., Epple, M., 2003. Early mineralization in *Biomphalaria glabrata*: Microscopic and structural results. J. Mollus. Stud. 69, 113–121.

Neues, F., Ziegler, A., Epple, M., 2007. The composition of the mineralized cuticle in marine and terrestrial isopods: a comparative study. Cryst. Eng. Comm. 9, 1245–1251.

Price, J.B., Holdich, D.M., 1980a. An ultrastructural study of the integument during the moult cycle of the woodlouse, *Oniscus asellus* (Crustacea, Isopoda). Zoomorphology 95, 250–263.

Price, J.B., Holdich, D.M., 1980b. The formation of the epicuticle and associated structures in *Oniscus asellus* (Crustacea, Isopoda). Zoomorphology 94, 321–332.

Raz, S., Weiner, S., Addadi, L., 2000. Formation of high-magnesian calcites via an amorphous precursor phase: possible biological implications. Adv. Mater. 12, 38–42.

Raz, S., Testeniere, O., Hecker, A., Weiner, S., Luquet, G., 2002. Stable amorphous calcium carbonate is the main component of the calcium storage structures of the crustacean *Orchestia cavimana*. Biol. Bull. 203, 269–274.

Reddy, M.M., 1977. Crystallization of calcium carbonate in the presence of trace concentrations of phosphorus-containing anions. J. Cryst. Growth 41, 287–295.

Roer, R., Dillaman, R., 1984. The structure and calcification of the crustacean cuticle. Am. Zool. 24, 893–909.

Romano, P., Fabritius, H., Raabe, D., 2007. The exoskeleton of the lobster *Homarus americanus* as an example of a smart anisotropic biological material. Acta Biomater. 3, 301–309.

Rutt, H.N., Nicola, J.H., 1974. Raman spectra of carbonates of calcite structure. J. Physiol. C 7, 4522–4528.

Schmalfuss, H., 1984. Eco-morphological strategies in terrestrial isopods. Symp. Zool. Soc. Lond. 53, 49–63.

Schmidt, U., Hild, S., Ibach, W., Hollricher, O., 2005. Characterization of thin polymer films on the nanometer scale with confocal Raman AFM. Macromol. Symp. 230, 133–143.

Shafer, T.H., Roer, R.D., Midgette-Luther, C., Brookins, T.A., 1995. Postecdysial cuticle alteration in the blue crab, *Callinectes sapidus*: Synchronous changes in glycoproteins and mineral nucleation. J. Exp. Zool. 271, 171–182.

Skinner, D.M., Kumari, S., O'Brien, J.J., 1992. Proteins of crustacean exoskeleton. Am. Zool. 32, 470–484.

Steel, C.G.H., 1993. Storage and translocation of integumentary calcium during the moult cycle of the terrestrial isopod *Oniscus asellus* (L.). Can. J. Zool. 71, 4–10.

Strus, J., Compere, P., 1996. Ultrastructural analysis of the integument during the moult cycle in *Ligia italica* (Crustacea, Isopoda). Eur. J. Physiol. 431, R251–R252.

Strus, J., Blejec, A., 2001. Microscopic anatomy of the integument and digestive system during the molt cycle in *Ligia italica* (Oniscidea). In: Kensley, B., Brusca, R.C. (Eds.), Isopod Systematcis and Evolution. Brookfield, pp. 343–352.

Sugawara, A., Nishimura, T., Yamamoto, Y., Inoue, H., Nagasawa, H., Kato, T., 2006. Self-organization of oriented calcium carbonate/polymer composites: effects of a matrix peptide isolated from the exoskeleton of a crayfish. Angew. Chem. Int. Ed. Engl. 45, 2876–2879.

Takagi, Y., Ishii, K., Ozaki, N., Nagasawa, H., 2000. Immunolocalization of gastrolith matrix protein (GAMP) in the gastroliths and exoskeleton of crayfish, *Procambarus clarkii*. Zool. Sci. 17, 179–184.

Testenière, O., Hecker, A., Le Gurun, S., Quennedey, B., Graf, F., Luquet, G., 2002. Characterization and spatiotemporal expression of orchestin, a gene encoding an ecdysone-inducible protein from a crustacean organic matrix. Biochem. J. 361, 327–335.

Tlili, M.M., Ben Amor, M., Gabrielli, C., Joiret, S., Maurin, G., Rousseau, P., 2001. Characterization of $CaCO_3$ hydrates by micro-Raman spectroscopy. J. Raman Spectrosc. 33, 10–16.

Vijayan, K.K., Diwan, A.D., 1996. Fluctuations in Ca, Mg and P levels in the hemolymph, muscle, midgut gland and exoskeleton during the moult cycle of the indian white prawn, *Penaeus indicus* (Decapoda: Penaeidae). Comp. Biochem. Physiol. 114A, 91–97.

Volkmer, D., Harms, M., Gower, L., Ziegler, A., 2005. Morphosynthesis of nacre-type laminated $CaCO_3$ thin films and coatings. Angew. Chem. Int. Ed. Engl. 44, 639–644.

Weiner, S., Levi-Kalisman, Y., Raz, S., Addadi, L., 2003. Biologically formed amorphous calcium carbonate. Connect. Tissue Res. 44 (Suppl 1), 214–218.

Weiss, I.M., Tuross, N., Addadi, L., Weiner, S., 2002. Mollusc larval shell formation: amorphous calcium carbonate is a precursor phase for aragonite. J. Exp. Biol. 293, 478–491.

Welinder, B.S., 1975. The crustacean cuticle: III composition in the individual layers in *Cancer pagurus* cuticle. Comp. Biochem. Physiol. 52A, 659–663.

Wood, S., Russell, J.D., 1987. On the nature of the calcium carbonate in the exoskeleton of the woodlouse *Oniscus asellus* L. (Isopoda, Oniscoidea). Crustaceana 53, 49–53.

Ziegler, A., 1994. Ultrastructure and electron spectroscopic diffraction analysis of the sternal calcium deposits of *Porcellio scaber* Latr. (Isopoda, Crustacea). J. Struct. Biol. 112, 110–116.

Ziegler, A., 1997. Ultrastructural changes of the anterior and posterior sternal integument of the terrestrial isopod *Porcellio scaber* Latr. (Crustacea) during the moult cycle. Tissue Cell 29, 63–76.

Ziegler, A., 2002. X-ray microprobe analysis of epithelial calcium transport. Cell Calcium 31, 307–321.

Ziegler, A., Altner, H., 1995. Are most numerous sensilla of terrestrial isopods hygroreceptors? Ultrastructure of the dorsal tricorn sensilla of *Porcellio scaber*. Cell Tissue Res. 282, 135–145.

Ziegler, A., Hagedorn, M., Ahearn, G.A., Carefood, T.H., 2007. Calcium translocations during the moulting cycle of the semiterrestrial isopod *Ligia hawaiiensis* (Oniscidea, Crustacea). J. Comp. Physiol. B 177, 99–108.